particles

IMPACT FACTOR 2.3

CITESCORE 3.0

Article

Simulation of a SiPM-Based Cherenkov Camera

Isaac Buckland, Riccardo Munini and Valentina Scotti

Special Issue

Advances in Space AstroParticle Physics: Frontier Technologies for Particle Measurements in Space, 2025 Edition

Edited by

Dr. Matteo Duranti and Dr. Valerio Vagelli

MDPI

https://doi.org/10.3390/particles8040096

particles

MDPI

Article

Simulation of a SiPM-Based Cherenkov Camera

Isaac Buckland [1], Riccardo Munini [1] and Valentina Scotti [2,*]

[1] INFN Trieste, Galleria Padriciano, 99, 34149 Trieste, TS, Italy; isaac.james.buckland@ts.infn.it (I.B.); riccardo.munini@ts.infn.it (R.M.)
[2] INFN Napoli, Strada Comunale Cinthia, 80126 Napoli, NA, Italy
* Correspondence: scottiv@na.infn.it

Abstract

Future space detectors for Ultra High Energy neutrinos and cosmic rays will utilize Cherenkov telescopes to detect forward-beamed Cherenkov light produced by charged particles in Extensive Air Showers (EASs). A Cherenkov detector can be equipped with an array of Silicon Photo-Multiplier (SiPM) pixels, which offer several advantages over traditional Photo-Multiplier Tubes (PMTs). SiPMs are compact and lightweight and operate at lower voltages, making them well-suited for space-based experiments. The SiSMUV (SiPM-based Space Monitor for UV-light) is developing a SiPM-based Cherenkov camera for PBR (POEMMA Baloon with Radio) at INFN Napoli. To understand the response of such an instrument, a comprehensive simulation of the response of individual SiPM pixels to incident light is needed. For the accurate simulation of a threshold trigger, this simulation must reproduce the current produced by a SiPM pixel as a function of time. Since a SiPM pixel is made of many individual Avalanche Photo-Diodes (APDs), saturation and pileup in APDs must also be simulated. A Gaussian mixture fit to ADC count spectrum of a SiPM pixel exposed to low levels of laser light at INFN Napoli shows a significant amount of samples between the expected PE (Photo Electron) peaks. Thus, noise sources such as dark counts and afterpulses, which result in partially integrated APD pulses, must be accounted for. With static, reasonable values for noise rates, the simulation chain presented in this work uses the characteristics of individual APDs to produce the aggregate current produced by a SiPM pixel. When many such pulses are simulated and integrated, the ADC spectra generated by low levels of laser light at the INFN Napoli SiSMUV test setup can be accurately reproduced.

Keywords: SiPM; simulation; Cherenkov

check for updates

Academic Editors: Armen Sedrakian, Matteo Duranti and Valerio Vagelli

Received: 12 September 2025
Revised: 17 November 2025
Accepted: 1 December 2025
Published: 3 December 2025

Citation: Buckland, I.; Munini, R.; Scotti, V. Simulation of a SiPM-Based Cherenkov Camera. *Particles* **2025**, *8*, 96. https://doi.org/10.3390/particles8040096

Copyright: © 2025 by the authors. Licensee MDPI, Basel, Switzerland. This article is an open access article distributed under the terms and conditions of the Creative Commons Attribution (CC BY) license (https://creativecommons.org/licenses/by/4.0/).

1. Introduction

SiPMs have been used in a variety of different applications in science, engineering, and medicine where counting of individual photons is needed. In the context of the detection of Cherenkov light produced by EASs, as with the PBR mission [1], to have accurate detector sensitivity and event reconstruction, a reliable simulation of the response of a SiPM-based telescope to incoming light is needed. This work uses the fundamental electrical characteristics of individual APDs in a SiPM pixel to construct an accurate simulation of the aggregate current produced when a SiPM pixel is exposed to low levels of light.

A SiPM pixel has many APDs coupled with quenching resistors, each of which constitutes a microcell. A schematic of multiple microcells is shown in Figure 1. Photo-Electrons (PEs) are released in a microcell with a probability based on the Photo-Detection Efficiency (PDE) of the SiPM, which is a function of the wavelength of the incoming photons. The PDE

versus photon wavelength for the Hamamatsu S13361-3050AE-08 MPPC (produced by the Hamamatsu corporation in Hamamatsu City, Shizuoka Prefecture in Japan) is shown in Figure 2. The S13361-3050AE-08 has 64 pixels, which are the data channels of the array.

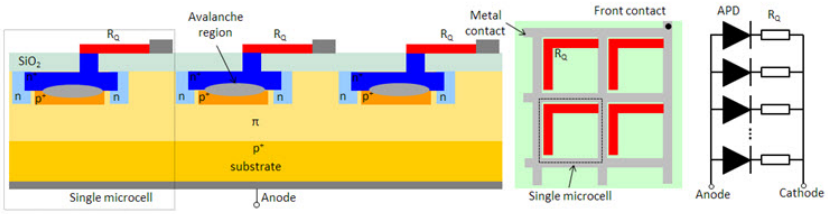

Figure 1. This figure from [2] shows a schematic of the microcells in a SiPM.

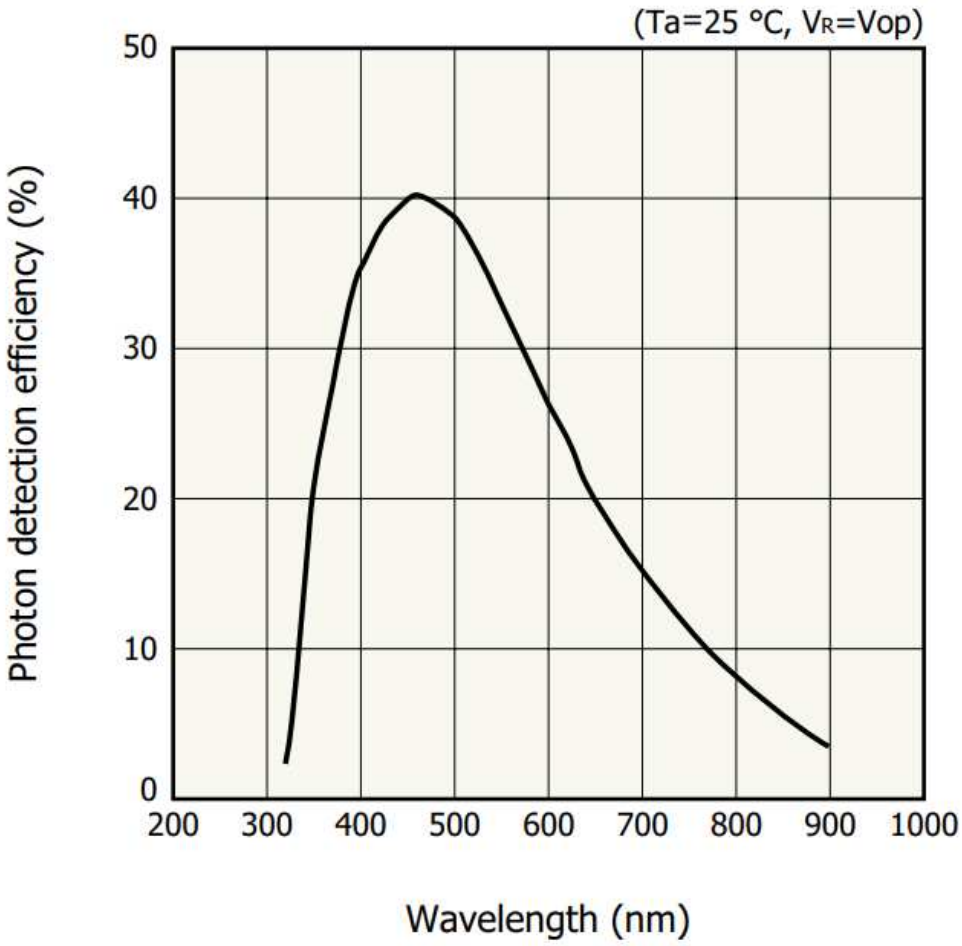

Figure 2. This figure from [3] shows the PDE response to photon wavelength for the Hamamatsu S13361-3050AE-08 MPPC.

The APD has an intrinsic capacitance C_{apd} and resistance R_{apd}, and when reverse-biased, a breakdown voltage V_{bd}. Thus, an idealized microcell is equivalent to adjacent Resistor–Capacitor circuits, where the other loop is made by the external voltage V_{bias}, quenching resistor R_q and C_{apd}. This circuit is shown in Figure 3.

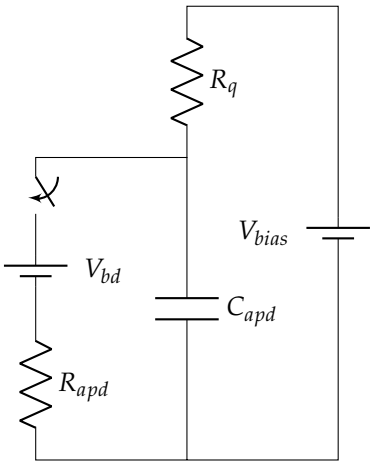

Figure 3. This figure shows the equivalent circuit to an APD. R_q is the quenching resistor, V_{bd} is the breakdown voltage, V_{bias} is the bias voltage, and R_{apd} and C_{apd} are the intrinsic APD resistance and capacitance, respectively.

Under a reverse-bias greater than the V_{bd}, the capacitance of the APD is charged and will undergo a full avalanche breakdown if a single PE is released, similar to closing a switch. This state is known as Geiger-mode, as each individual PE produces a full breakdown. If a photon releases a PE in the avalanche region of an APD, the "switch" is closed and C_{apd} discharges across R_{apd}, inducing an increasing voltage drop across R_q. The current increases until the probability of impact ionization of electrons in the avalanche is small enough so no current flows inside the apd. This occurs at approximately a maximum current I_{max} given by Equation (1). At this point, the avalanche quenches (closing the "switch") and C_{apd} is recharged and it returns to Geiger-mode. The difference between the bias voltage and the breakdown voltage is the overvoltage. The gain of the SiPM increases linearly with overvoltage in its working region (between 2 and 8 Volts in the case of the Hamamatsu S13361-3050AE-08 [3]) and is thus the primary controllable factor for tuning the gain.

$$I_{max} \approx \frac{V_{bias} - V_{bd}}{R_q + R_{apd}} \tag{1}$$

Thus, the shape of an individual pulse is characterized by three parameters: the discharge time constant $\tau_d = R_{apd}C_{apd}$, the recharge time constant $\tau_r = R_qC_{apd}$, and the peak time after the PE release t_{max} which occurs when the current reaches I_{max}. This functional form is defined in Equation (2).

$$I(t) = I_{max}\begin{cases} 1 - e^{\frac{-t}{\tau_d}}, & t < t_{max} \\ e^{\frac{-(t-t_{max})}{\tau_r}}, & t \geq t_{max} \end{cases} \tag{2}$$

Since one pixel in a SiPM contains a finite number of microcells (3584 in the case of the Hamamatsu S13361-3050AE-08), there is always the possibility (increasing with PE released in the pixel) that two or more PEs are released in the same microcell. If the PEs released in a SiPM pixel are equally likely to occur in any microcell, it is possible to calculate the distribution of microcells with multiple PEs for a given number of released PEs. If each PE is assigned a random microcell, each microcell with at least one PE can be counted. This was performed 10,000 times and the resulting histograms for increasing numbers of released PEs is shown in Figure 4. Since up to hundreds of photons could be expected from Cherenkov events to be focused on a single pixel [4], the effect of microcell saturation is non-negligible.

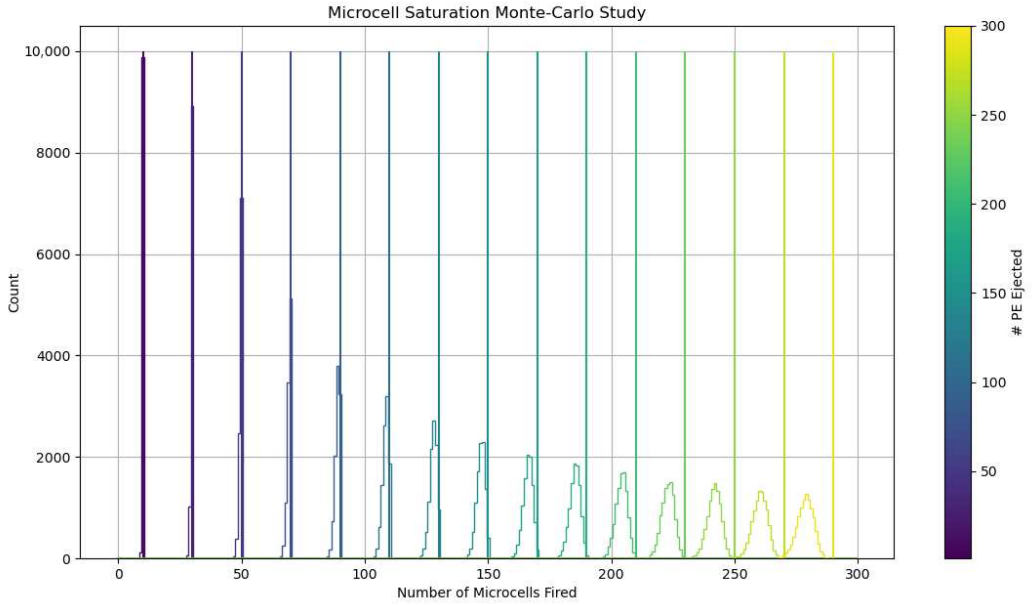

Figure 4. This figure shows the distribution of microcells with at least one PE in the Hamamatsu S13361-3050AE-08 for increasing numbers of released PEs randomly assigned to microcells. The vertical lines to the right of the histograms, and in the same color, lie on the number of PEs which were used to generate the corresponding distributions.

If another charge carrier (PE or otherwise) is released while the APD is recharging, it can only discharge what has accumulated in C_{apd} up to that point. Also, if another PE is released during the avalanche, the current flowing across the terminals of the microcell is unaffected. Thus, if two or more PEs are released in the same microcell within the time frame of a single pulse, the current output will be different depending on when a PE release occurs relative to the previous one. An idealized current response to released PE is shown in Figure 5. In actual SiPMs, both the dark current (baseline) and the total charge of an avalanche breakdown have statistical variance.

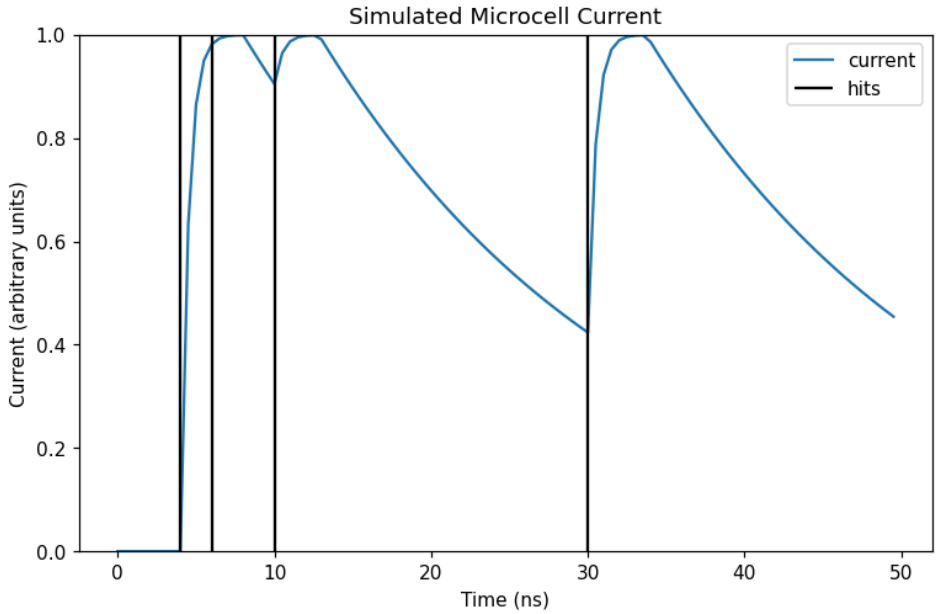

Figure 5. This figure shows the idealized current response of a single microcell to multiple PEs.

A SiPM has several sources of spurious pulses. In the absence of light, occasionally a charge carrying particle can be released in an APD avalanche region due to thermal excitation. The rate of these so-called dark counts depends exponentially on the temperature [5]. The dark count rate initially depends linearly on the overvoltage for the first few volts, then exponentially afterwards [5]. In the case of the Hamamatsu S13361-3050AE-08, the dark count rate is between 0.5 and 1.5 MHz at 25 °C and an overvoltage of 3 Volts [3]. The dark count rate for this MPPC was measured to be 0.7 MHz at 19.5 °C at an overvoltage of 3.55 Volts by [6]. Also, any time an APD undergoes avalanche breakdown (for any reason) photons can propagate to neighboring microcells and cause them to undergo avalanche breakdown at nearly the same time [5]. The probability of crosstalk depends on the geometry of microcells relative to each other in the pixel, and the overvoltage [2]. Finally, charge carriers can be temporarily trapped by impurities in the silicon near the avalanche region, re-releasing those charge carriers and thus re-triggering the APD after some time has passed [5]. This is known as afterpulsing. Both crosstalk and afterpulses are correlated noise, meaning their level depends on the incoming signal.

2. Materials and Methods

This section describes the lab setup at INFN Napoli, Strada Comunale Cinthia, 80126 Napoli NA, Italy, the methods used to analyze the data from that setup, and the simulation procedure used to reproduce that data.

2.1. Test Setup at INFN Napoli

The INFN laboratory in Napoli has constructed a test setup for the Hamamatsu S13361-3050-NE-08 64 channel MPPC to characterize the gain, crosstalk and afterpulse probability, and PDE. An integrating sphere was coupled to a 405 nm laser and a calibrated photodiode. The photodiode gives a reference value for the amount of light exposed to the SiPM. A fiber optic cable from an opening on the integrating sphere is routed to a 3-axis movement system which allows illumination of any individual pixel in the matrix. The SiPM bias voltage, the digitization of integrated SiPM signals (for an integration time of 80 ns), and the external trigger (activated at the same time as the input laser) are all controlled by a prototype acquisition board. This board comprises a RADIOROC ASIC by Weeroc, a Xilinx Artix 7 FPGA, and a CAEN A7585DU module. The whole test setup is contained in a dark box. A detailed description of the setup is provided in [7].

2.2. Gaussian Mixture Fit

In order to understand the distributions of integrated pulse values from the test setup, a global fit to all the photoelectron peaks, known as a "finger plot" (Figure 6), is performed using the method of expectation maximization. As long as the pulse is not truncated, the number of ADC counts recorded for a given number of PE is a Gaussian distributed random variable. Thus, a reasonable Probability Density Function (PDF) from which all data in an acquisition is drawn is given by Equation (3), where $P_j(\vec{X}|\sigma_j, \mu_j)$ is a standard Gaussian and π_j is the relative contribution of peak j. A fit of the data to this PDF yields parameters $\vec{\mu}$, $\vec{\sigma}$, and $\vec{\pi}$ for each peak.

$$P(\vec{X}|\hat{\theta}) = \sum_{j=1}^{M} \pi_j P_j(\vec{X}|\sigma_j, \mu_j) \tag{3}$$

While photoelectron peaks are mostly easy to distinguish visually, enough overlap exists between the peaks such that the specific number of PE which generated a given sample value is not known a priori. Therefore a sum exists in the argument of the logarithm in the expression for the log-likelihood, making it not easily differentiable. Instead, the ex-

pectedvalue of the log likelihood is used to construct estimators for all of the Gaussian peak parameters. The expected value is the sum of the average log-likelihood contributions of each sample given a prior set of parameters $\vec{\mu}$, $\vec{\sigma}$, and $\vec{\pi}$. This requires reasonable estimates for the probability that each sample is drawn from each peak, which are computed using Bayes' rule with guesses for the peak proportions $\vec{\pi}$ as the priors. Thus, parameter values obtained from the estimators can be used to recompute better probabilities, and subsequently better parameter values from the estimators. This algorithm was implemented for a one dimensional sample using python. A more detailed description, and the algorithm itself, can be found in the "EM Gaussian mixture" v1.0.0 GitHub repository [8].

When ADC sample distributions are fit using expectation maximization, a higher value for the log likelihood is obtained when the number of peaks j is allowed to be one more than the number of visually resolvable peaks compared to just the number of peaks. This is because truncated dark counts and afterpulses (cut at the end of the integration window), and pileup pulses in saturated microcells result in pulse areas not drawn from the Gaussian for a given peak. Since this contribution is non-negligible, the fit results in an additional wide peak around the centroid of the PE peaks. A Gaussian mixture fit with one more peak than the PE peaks is shown in Figure 6. Any simulation must produce these anomalous samples to produce an accurate trigger rate. Also, in order to estimate the variance of an integrated single PE pulse, this noise must be excluded.

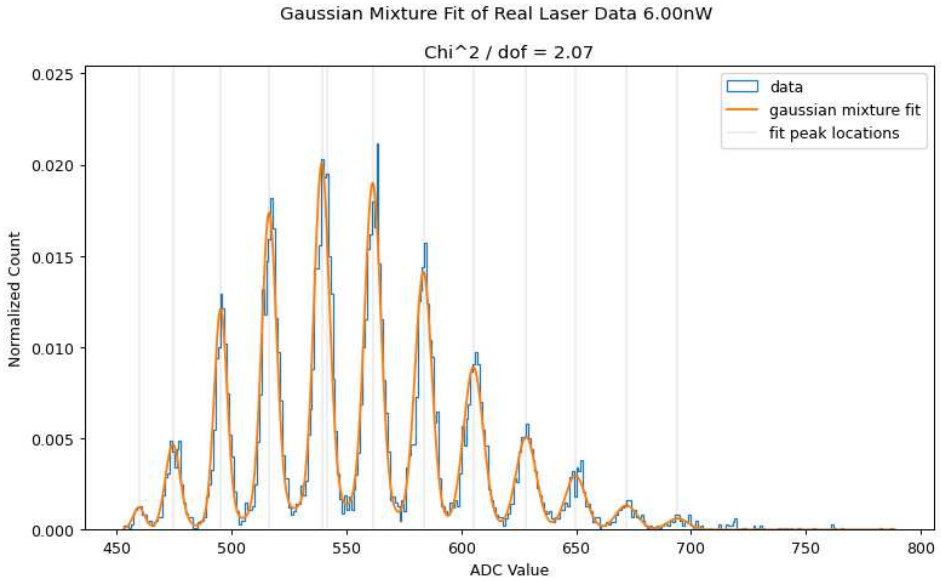

Figure 6. This figure is a histogram of 10,000 integrated ADC count values from a data acquisition run from the Napoli test setup. This acquisition was performed using 6 nW of power supplied to the 405 nm laser. A Gaussian mixture fit yielded a χ^2/ndf of 2.07.

The gain of the SiPM, in ADC counts per PE, is determined by a linear fit of the PE peaks their corresponding ADC values. This fit is shown in Figure 7. The value of the gain is 22.05 ± 0.06 ADC counts per PE.

2.3. Simulation of SiPM Response in EUSO-OffLine

The simulation of the behavior of the SiPM pixels and their response to incoming light was implemented as a module in the JEM-EUSO version of the OffLine cosmic ray detector simulation framework. OffLine is a modular framework written in modern C++ [9].

Other existing SiPM simulations account for some, but not all, of the characteristics simulated in this work. The SiPM simulation presented in [10] takes into account microcell saturation but not the interplay between a saturating level of PEs, crosstalk, and after-

pulsing. With the simulation of individual APDs, the pile-up current resulting from such saturated microcells is simulated in this work. The simulation framework presented in [11] reproduces ADC distributions (finger plots) and was used for the hypothetical simulation of an IACT (Imaging Atmospheric Cherenkov Telescope), but does not output the current trace of a SiPM. The simulation procedure presented in this section does produce SiPM current as a function of time.

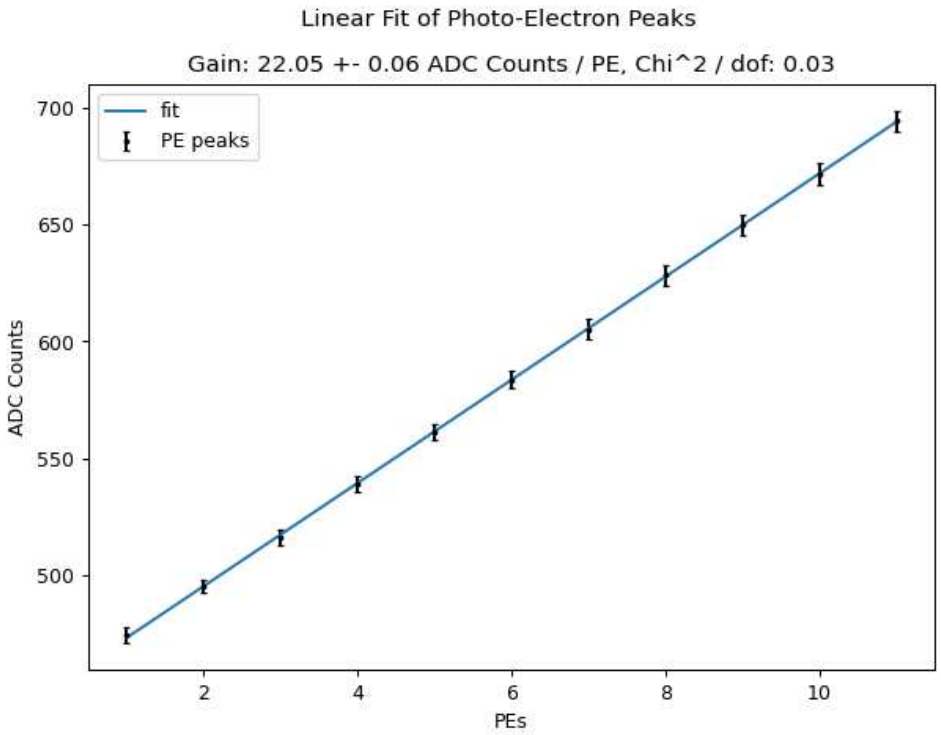

Figure 7. This figure shows the linear fit to ADC counts at each PE peak.

In the final implementation, simulated photons traced from outside the telescope, off the mirror, and to pixels in the Cherenkov camera will serve as the inputs for the module. However, for the single-pixel simulation, a Poisson-distributed random number of 405 nm wavelength photons, the mean of which reflects the power of the laser, is assigned to a single pixel. The relative PE peak heights in Figure 6 were fit to a Poisson distribution to estimate the mean number of PEs in a sample (4.57 ± 0.02 PEs). The mean dark counts expected in a sample (0.12 PEs) were subtracted, and the PDE at 405 nm is applied to estimate a mean number of photons incident on the SiPM from the laser (12.37 photons). The arrival time of these photons is drawn from a Gaussian centered at 20 ns, with a sigma of 5 ns, after the start of the 80 nanosecond integration time of the ASIC. Each photon, within OffLine, has a wavelength, time, and weight.

The SiPM pixel module starts initializing two C++ deques. One for the PE release times, and one for the index of the microcell in which it is released. First, the number of dark counts occurring during the integration time is simulated by drawing a number of PE from a Poisson distribution. The dark count rate was estimated by a Poisson fit to the relative heights of the PE peaks in the pedestal data. Each drawn dark count is assigned a uniformly distributed random time and a random microcell. Next, the photons incident on the pixel are simulated. The PDE at the wavelength of each photon is calculated by interpolation within the PDE curve shown in Figure 2. A PE release is simulated randomly with a probability of the PDE for each photon. All released PEs are added to the deque and assigned a random microcell index.

Since any avalanche breakdown is equally likely to cause correlated noise, the likelihood that avalanches caused by crosstalk and afterpulses cause more crosstalk and afterpulses must be taken into account. This is performed using a recursive function call. For a given avalanche (PE) occurring at a given time in a given microcell, first, crosstalk is simulated according to the crosstalk probability. If crosstalk occurred, another "PE" is added to the deques at the same time as the initial one in a random microcell, and the recursive function is called for the crosstalk pulse. Then (for the initial PE and first call to the recursive function), an afterpulse is simulated according to the afterpulse probability. If an afterpulse occurs, a "PE" is added to the deques with the same microcell index and at an exponentially distributed time after the initial PE. The recursive function is then called on the afterpulse. In this work, the PDE and crosstalk rate were taken from the datasheet for the S13361-3050AE-08 MPPC, while the afterpulse rate and baseline pixel current variance were set at reasonable values for other SiPMs based on other studies [5,6]. In a final, more complete Cherenkov camera simulation, directly measured values of these quantities for each pixel will be stored in the configuration files used by OffLine.

Once all the avalanches have been collected, the set of all microcells with at least one "PE" is compiled. For each one of these microcells, a value for the pedestal is drawn based on the measured mean an variance of the pedestal peak in Figure 8. Next, a baseline current with Gaussian noise is generated. Then, a pulse size for that microcell is drawn from a Gaussian with a mean at the gain (in ADC counts per PE) and a variance determined from the difference in the variance of the first PE peak and the pedestal. Finally, the current pulse shapes are generated. For each APD with at least one released "PE", the current pulse shapes are added. For APDs with multiple "PEs", if a subsequent "PE" arrives before the previous avalanche had quenched (before T_{max}) the pulse is unchanged. If a subsequent "PE" arrives after the previous avalanche had quenched and its pulse is decaying (the APD is recharging) the base current pulse, Equation (2), restarts from that current level. The current contributed from each APD is added to the baseline. The integrated signal is then calculated by a trapezoid sum on the aggregate current. The current, integrated signal, and simulated noise counts are all saved to the OffLine event data structure.

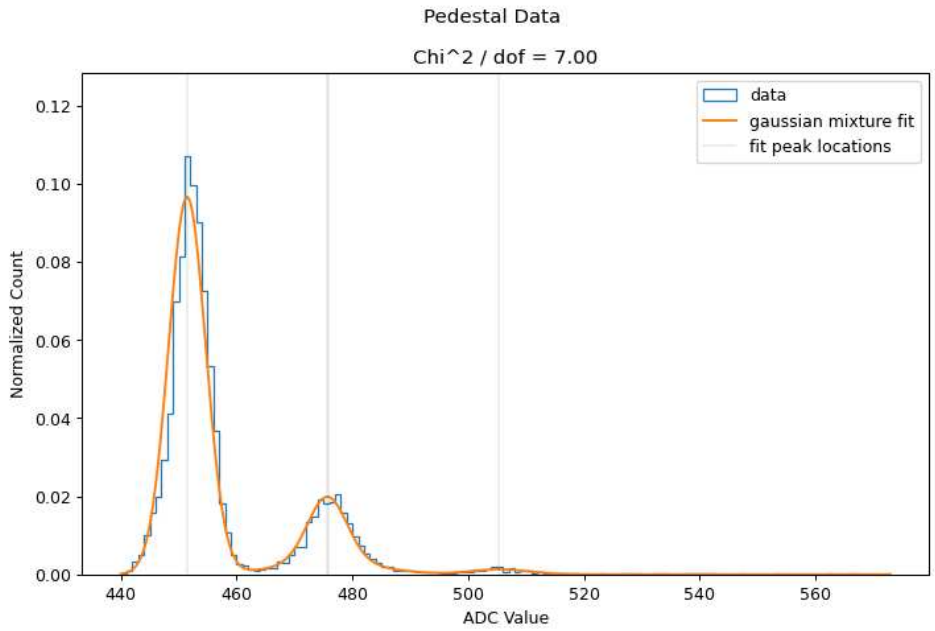

Figure 8. This figure is a histogram of 10,000 integrated ADC count values from a dark acquisition run from the Napoli test setup. The Gaussian mixture fit yielded a χ^2/ndf of 7.00.

3. Results

The method of simulation presented in this work reproduces the results of qualifying datasets for the SiSMUV modular UV detection module reading out the signal of the Hamamatsu S13361-3050AE-08 MPPC. Although PEs released from laser light are expected to produce fully integrated pulses, Figure 9 shows that both the individual Gaussian PE peaks and samples falling between PE peaks due to dark counts and afterpulses are generated by the simulation chain. Recursive calls to the crosstalk and afterpulse simulation accounts for all correlated noise. Also, the random microcell assignment and subsequent individual microcell current simulation accounts for saturation effects. An Epps–Singleton two-sample test [12] was performed comparing the laser data and simulated data. The test yielded that the simulated distribution could have resulted from the same underlying distribution as the laser data with a probability of 0.84.

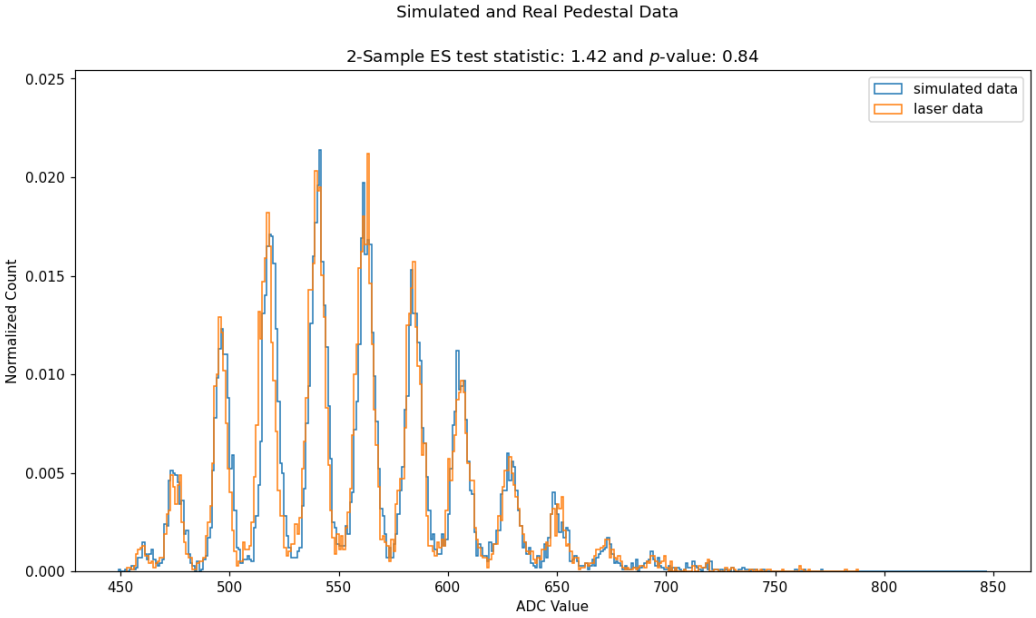

Figure 9. This figure is a histogram of two samples of 10,000 integrated ADC counts. One is from a data acquisition run from the Napoli test setup using 6 nW of power supplied to the 405 nm laser, and the other was simulated using the method described in this work.

4. Discussion

A detailed model of the response of a SiPM to incident light reduces the systematic uncertainties of future experiments using SiPM-based Cherenkov cameras. This work presents the current state of an simulation of the response of SiPM pixels to incident light developed for the SiSMUV project. The simulation can produce samples from the same underlying distribution as the laser data from INFN Napoli. Future tuning of the simulation will include the dependence of the gain and noise rates on overvoltage. Also, variations in SiPM characteristics due to changes in pressure and temperature will be included based on measurements performed by the greater PBR collaboration.

Author Contributions: Conceptualization, I.B., R.M., and V.S.; methodology, I.B., R.M., and V.S.; software, I.B.; validation, I.B., R.M., and V.S.; formal analysis, I.B.; investigation, I.B. and V.S.; resources, R.M. and V.S.; data curation, V.S.; writing—original draft preparation, I.B.; writing—review and editing, I.B.; visualization, I.B.; project administration, R.M. and V.S.; funding acquisition, R.M. and V.S. All authors have read and agreed to the published version of the manuscript.

Funding: This work was funded by the Italian Ministry of University and Research as a PRIN project under Grant CUP E53D23000610001.

Data Availability Statement: The raw data supporting the conclusions of this article will be made available by the authors upon request.

Acknowledgments: Gracious thanks are extended to the INFN staff in Trieste for assisting with the logistical difficulties of relocating to Italy.

Conflicts of Interest: The authors declare no conflicts of interest.

Abbreviations

The following abbreviations are used in this manuscript:

SiPM	Silicon Photo-Multiplier
PMT	Photo-Multiplier Tube
MPPC	Multi-Pixel Photon Counter
PDE	Photon Detection Efficiency
APD	Avalanche Photo-Diode
PE	Photo-Electron

References

1. Eser, J.; Olinto, A.V.; Osteria, G. POEMMA-Balloon with Radio: An Overview. In Proceedings of the 39th International Cosmic Ray Conference ICRC2025, Geneva, Switzerland, 15–24 July 2025; p. 249.
2. Piatek. *What Is an SiPM and How Does It Work?* 2016. Available online: https://hub.hamamatsu.com/us/en/technical-notes/mppc-sipms/what-is-an-SiPM-and-how-does-it-work.html (accessed on 1 April 2025).
3. Hamamatsu. *MPPC (Multi Pixel Photon Counter) Arrays*; S13361-3050 Series; Hamamatsu 1126-1, Ichino-cho, Chuo-ku, Hamamatsu City, Shizuoka Pref., 435-8558, Japan. 2024. Available online: https://www.hamamatsu.com/content/dam/hamamatsu-photonics/sites/documents/99_SALES_LIBRARY/ssd/s13361-3050_series_kapd1054e.pdf (accessed on 1 April 2025).
4. Reno, M.H.; Krizmanic, J. *ν*SpaceSim: A Comprehensive Simulation Package for Modeling the Measurement of Cosmic Neutrinos using the Earth as the Neutrino Target and Space-based Detectors. In Proceedings of the 39th International Cosmic Ray Conference ICRC2025, Geneva, Switzerland, 15–24 July 2025; p. 1082.
5. Vacheret, A.; Barker, G.J.; Dziewiecki, M.; Guzowski, P.; Haigh, M.D.; Hartfiel, B.; Izmaylov, A.; Johnston, W.; Khabibullin, M.; Khotjantsev, A.; et al. Characterization and simulation of the response of Multi-Pixel Photon Counters to low light levels. *NIMA* **2011**, *1*, 69–83. [CrossRef]
6. Renschler, M.; Painter, W.; Bisconti, F.; Haungs, A.; Huber, T.; Karus, M.; Schieler, H.; Weindl, A. Characterization of Hamamatsu 64-channel TSV SiPMs. *Nucl. Instrum. Methods Phys. Res. Sect. A Accel. Spectrometers Detect. Assoc. Equip.* **2018**, *888*, 257–267. [CrossRef]
7. Scotti, V.; Anastasio, A.; Boiano, A.; Buckland, I.; Masone, V.; Mese, M.; Munini, R. SiSMUV: A modular UV detector for space telescopes using SiPM. In Proceedings of the 39th International Cosmic Ray Conference ICRC2025, Geneva, Switzerland, 15–24 July 2025; p. 390.
8. Isaac Buckland. *Fitting a Gaussian Mixture (in 1-Dimension) Using Expectation Maximization (EM)*. Available online: https://github.com/ikepc1/EM_Gaussian_Mixture (accessed on 30 August 2025) .
9. Eser, J. EUSO-Offline: A comprehensive simulation and analysis framework. *J. Instrum.* **2024**, *19*, P01007. [CrossRef]
10. Acerbi, F.; Gundacker, S. Understanding and simulating SiPMs. *Nucl. Instrum. Methods Phys. Res. Sect. A Accel. Spectrometers Detect. Assoc. Equip.* **2019**, *926*, 16–35. [CrossRef]
11. Peña-Rodríguez, J.; Förtsch, J.; Pauly, C.; Kampert, K.-H. A Simulation Framework for APD, SiPM, and MPPCs. Available online: https://arxiv.org/html/2411.16710v1 (accessed on 30 August 2025).
12. Epps, T.W.; Singleton, K.J. An omnibus test for the two-sample problem using the empirical characteristic function. *J. Stat. Comput. Simul.* **1986**, *26*, 177–203. [CrossRef]

Disclaimer/Publisher's Note: The statements, opinions and data contained in all publications are solely those of the individual author(s) and contributor(s) and not of MDPI and/or the editor(s). MDPI and/or the editor(s) disclaim responsibility for any injury to people or property resulting from any ideas, methods, instructions or products referred to in the content.